



Article

# Composite of Cellulose-Nanofiber-Reinforced Cellulose Acetate Butyrate: Improvement of Mechanical Strength by Cross-Linking of Hydroxyl Groups

Romain Milotskyi \*, Ryo Serizawa, Kaoru Yanagisawa, Gyanendra Sharma, Elisabeth Rada Desideria Ito, Tetsuo Fujie, Naoki Wada \* and Kenji Takahashi

Institute of Science and Engineering, Kanazawa University, Kakuma machi, Kanazawa 920-1192, Japan

\* Correspondence: romain-mi@se.kanazawa-u.ac.jp (R.M.); naoki-wada@se.kanazawa-u.ac.jp (N.W.)

**Abstract:** A great challenge hindering the use of cellulose nanofibers (CNF) as a reinforcing filler in bio-based polymeric matrices are their poor chemical compatibility. This is because of the inherent hydrophilic nature of CNF and the hydrophobic nature of the polymeric matrix. In this study, cellulose laminates were prepared by using CNF as a filler and cellulose acetate butyrate (CAB) as the polymer matrix. To improve the compatibility between CAB and CNF, the residual hydroxyl groups of CAB and the hydroxyl groups on the surface of CNF were cross-linked with bio-derived polyisocyanurate D376N (STABiO™). The composite material was obtained in one step by sandwiching a CNF sheet (10 wt%) coated with a cross-linking agent between CAB films (90 wt%) using hot pressing. When 14.3 wt% of the cross-linking agent to the total weight of CNF and CAB was added, the tensile strength and flexural strength were improved by 72.4% and 16.3%, respectively, compared with neat CAB. It was concluded that this increase in strength is a result of both: cross-linking between the CNF sheets as well as the cross-linking occurring at the CNF/CAB interface.

**Keywords:** composite material; cellulose ester; CNF; mechanical strength; cross-linking; urethane bond



**Citation:** Milotskyi, R.; Serizawa, R.; Yanagisawa, K.; Sharma, G.; Ito, E.R.D.; Fujie, T.; Wada, N.; Takahashi, K. Composite of Cellulose-Nanofiber-Reinforced Cellulose Acetate Butyrate: Improvement of Mechanical Strength by Cross-Linking of Hydroxyl Groups. *J. Compos. Sci.* **2023**, *7*, 130. <https://doi.org/10.3390/jcs7030130>

Academic Editor: Francesco Tornabene

Received: 22 February 2023

Revised: 10 March 2023

Accepted: 16 March 2023

Published: 22 March 2023



**Copyright:** © 2023 by the authors. Licensee MDPI, Basel, Switzerland. This article is an open access article distributed under the terms and conditions of the Creative Commons Attribution (CC BY) license (<https://creativecommons.org/licenses/by/4.0/>).

## 1. Introduction

Composite materials made from a polymer matrix and a reinforcement synthetic filler (e.g., glass fiber, carbon fibers) play a dominant role in various applications (automotive, packaging, fashion). However, the synthetic nature of composite components causes difficulties for end-life disposal of these materials. In contrast, biocomposites produced from a bio-based filler and bio-based matrix are a great attraction, which can present desired functionalities at a reasonable cost [1]. Compared with synthetic fibers, natural fibers have many advantages due to their abundance, low density, and low cost. Particularly, cellulose nanofibers (CNF) were recently applied to create new biocomposite materials. In one study, CNF derived from Kenaf were combined with a polylactic acid (PLA) matrix [2]. The final material showed higher tensile strength as well as a significant increase in thermal stability compared with pure PLA. In another study, chitosan was reinforced with CNF [3]. The obtained composite showed great acid-resistant properties (95% acid-resistant degree) and excellent recyclability (approximately 85% desorption rate) after five recycles of adsorption–desorption. However, a homogeneous dispersion of CNF in a biopolymer matrix is required for obtaining composite materials with higher mechanical properties and consistent performance [4]. Aggregation of the dispersed phase may cause bond weakening which in turn affects the mechanical properties of the resultant composite material as aggregates act as stress concentrators [5]. A typical example would be the inherent chemical incompatibility between a hydrophilic CNF and a hydrophobic polymer matrix which is a reason for a weak interfacial bonding between the CNF and biopolymer components. The compatibility can be improved by a chemical modification of the fiber surface. Some of the

cellulose surface modification techniques include acetylation [6,7], chemical grafting [8,9], and silylation [10–12].

In addition to the fibers, the use of a continuous polymer matrix phase is crucial because the matrix transfers stress between fibrils, reduces moisture sorption, allows composite shaping, and provides the opportunity for property tailoring [13]. Several thermoplastic cellulose derivatives, including cellulose acetate (CA), cellulose acetate propionate (CAP), and cellulose acetate butyrate (CAB), are widely used as bio matrices for composite materials [14,15]. In this case, it is possible to prepare the composite using a dry process by direct compounding (extrusion) of cellulose thermoplastic derivative and nanocellulosic filler [16]. Furthermore, the composite material can be obtained by a wet process in which cellulose nanofibers and a cellulose thermoplastic matrix are dispersed and dissolved in an organic solvent and the solvent is volatilized [17]. However, in both cases, to produce the final shape material, injection molding is often carried out. Additionally, until now, the researchers focused mainly on achieving high mechanical properties and additional functionality of composite materials rather than process development efficiency [18]. The challenge today is to develop a simple process (1–2 steps) of cellulose composite manufacture. At the same time, the obtained cellulose composite should present improved mechanical performance, high porosity, and good compatibility between matrix and reinforcement filler.

Therefore, in this study, we attempted to fabricate sandwich material from bamboo-derived CNF and CAB directly by hot pressing, which is another molding method. Moreover, polyisocyanurate (D376N) was added to convert the hydroxyl groups remaining in the cellulose thermoplastic, and the hydroxyl groups present on the CNF surface, into urethane bonds. The CAB/CNF/D376N system can form covalent cross-links, which will enhance the interaction between the matrix and the fibers. This improved interaction will in turn prevent the two components from delamination, which will enhance the mechanical properties. The applied polyisocyanurate derives from biomass and has the advantage of not generating by-products when hydroxyl groups and isocyanate groups react to form urethane bonds and is environmentally friendly from the viewpoint of volatile organic compound emissions. Process parameters (hot-press pressure, time) were studied to find optimal conditions. The cross-linking between CNFs and at the CNF/CAB interface was investigated.

## 2. Materials and Methods

### 2.1. Materials

Cellulose acetate butyrate CAB500-5 was purchased from Eastman Chemical Company, Kingsport, TN, USA. CAB500-5 was reported to have the following properties: number average molecular weight of 57,000 Daltons, DS (butyryl) 2.73, DS (acetyl) 0.02 and 0.25 of free OH groups. Nanoforest-S low-defibrillated bamboo CNF were obtained from Chuetsu Pulp and Paper Co., Ltd., Takaoka, Japan. Cross-linking agent polyisocyanurate D376N (STABIO™) (Scheme S1) was provided by Mitsui Chemicals, Japan. All other chemicals were provided by Tokyo Chemical Industry Co., Ltd. (Tokyo, Japan). All chemicals were used as received without any further purification.

### 2.2. Samples Preparatio

Untreated CNF sheet preparation. An amount of 30 g of a 1.7 wt% aqueous dispersion of bamboo CNF was placed in a 2 L beaker and 1 L of distilled water was added and stirred for 30 min to obtain a 0.05 wt% CNF water dispersion. Then, the obtained dispersion was vacuum filtrated through a membrane filter (cellulose mixed ester, pore size 0.45  $\mu\text{m}$ ). Next, the entire membrane filter was removed and hot pressed using a manual hydraulic heating press (Imoto Manufacturing Co., Ltd., Osaka, Japan) to remove excess of water. More specifically, the CNF sheet was sandwiched between a cellulose ester membrane filter, filter paper (AFSIL), and a PTFE-impregnated glass fabric sheet on a 170 mm  $\times$  170 mm stainless steel plate from each side. The filter paper was used for moisture absorption. The sheets were then hot pressed at 70  $^{\circ}\text{C}$  for 10 min with a force of 5 kN. After the hot pressing,

a 10 kg weight was placed on the sheet for 1 min at room temperature to cool it, and the membrane filter and other components were slowly peeled off to obtain the CNF sheet. The obtained CNF sheets were dried under vacuum at 100 °C for 20 h. CNF sheets with thicknesses of 32–44 µm and Φ142 mm were then obtained. The scheme of untreated CNF sheets preparation is available in Supplementary Information (Scheme S2).

**Acetone-treated CNF (A-CNF) sheet preparation.** An amount of 30 g of a 1.7 wt% aqueous dispersion of bamboo CNF was placed in a 2 L beaker and 1 L of distilled water was added and stirred for 30 min to obtain a 0.05 wt% CNF water dispersion. Then, the obtained dispersion was vacuum filtrated through a membrane filter (cellulose mixed ester, pore size 0.45 µm). However, after vacuum filtration, the CNF sheet was immediately removed from the membrane filter and was soaked in 150 mL of acetone for 2 h and, after changing to fresh acetone, the solution was left for another 24 h to swell the CNF sheet. CNF sheets were then hot pressed between filter paper (AFSIL) and a PTFE-impregnated glass fabric sheet on a 170 mm × 170 mm stainless steel plate from each side at 70 °C for 10 min with a force of 5 kN. The obtained CNF sheets were dried under vacuum at 100 °C for 20 h (Scheme S3).

**CAB/A-CNF lamination.** Laminated materials of A-CNF sheets and CAB sheets (10 wt% vs. 90 wt%, respectively) were prepared by applying a 15 wt% mixture of D376N dissolved in THF to the CNF sheets and allowing the THF to volatilize (Figure 1). The concentration of the cross-linker was 0, 3.9, 7.7, 14.3, and 24.5 wt% with respect to the total weight of CNF and CAB. The two CAB sheets and the A-CNF sheet with cross-linker were then laminated using a hot-press machine. The forming process conditions included preheating at 190 °C and 0 kN for 5 min, followed by forming at the same temperature for 15 min at 20 kN. The temperature of 190 °C was chosen based on CAB offset temperature + 15 °C (Table S1). The test specimens were then cut out with reference to JISK7162-AB.

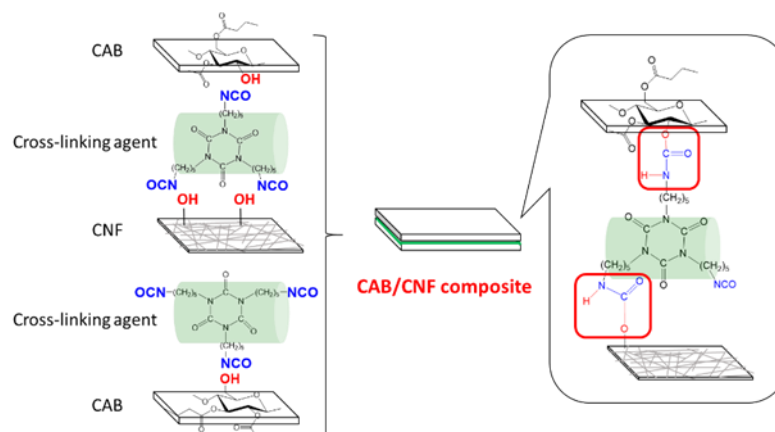


**Figure 1.** CAB/A-CNF composite material development.

**Strengthening of A-CNF by reaction with a cross-linking agent.** We investigated whether the addition of a cross-linking agent causes cross-linking between A-CNFs. Specifically, 348 mg of cross-linking agent D376N was dissolved in 2 g of THF, the resulting mixture was applied to CNF sheets, and the reaction was performed under the same hot-pressing conditions as in “CAB/A-CNF lamination”. The presence or absence of reaction was confirmed by ATR-FTIR spectroscopy measurement, and its mechanical strength was measured using a tensile test machine.

**CAB500-5 acetylation.** To examine the effect of the remaining hydroxyl groups of CAB, completely substituted CAB (CAB500-5 (DS 3)) was synthesized. For instance, 6 g of CAB500-5 was added into a 1 L Schlenk flask. The Schlenk flask was then filled with argon gas. Then, 360 mL of dehydrated THF was added to completely dissolve CAB500-5. After CAB500-5 was completely dissolved, acetic anhydride was added [7 eq./0.25 OH]. At the same time, DMAP was added [7 eq./0.25 OH]. The reaction was carried out at room

temperature for 24 h with stirring. After the reaction was completed, the THF was removed using an evaporator until the reaction solution was reduced to approximately 200 mL. Next, the reaction solution was dropped into 4.5 L of methanol and re-precipitated. The solution was then stirred for 1 h and filtered through 4C cellulose filter paper. After filtration, the resulting material was dissolved in 200 mL of dichloromethane and re-precipitated in 3 L of methanol, vacuum filtrated, and dried in a vacuum oven at 70 °C for 24 h.

### 2.3. Samples Characterization

Capillary rheometer measurements. Thermal flowability tests were conducted using a constant test force extrusion-type narrow-tube rheometer flow tester CFT-500EX (Shimadzu Corporation, Kyoto, Japan). A sample of 1 g was filled into a cylinder and extruded through a  $\Phi 1 \text{ mm} \times 10 \text{ mm}$  die by applying a force of 50 N with a piston area of  $1 \text{ mm}^2$  from the top while the temperature was increased at a rate of  $3 \text{ }^\circ\text{C}/\text{min}$ . The temperature at which the sample (cellulose derivative) begins to soften, the softening temperature ( $T_s$ ), the outflow start temperature ( $T_{fb}$ ), the melting temperature (offset temperature) ( $T_{\text{offset}}$ ), and the measurement end temperature ( $T_{\text{end}}$ ) were observed. Table S1 shows the thermal characteristics of CAB500-5 used in this study.

Thermogravimetric analysis (TGA). TGA measurements were performed on a Shimadzu DTG-60AH thermal analyzer (Shimadzu Co., Kyoto, Japan) using a temperature range from 50 to 600 °C at a heating rate of  $20 \text{ }^\circ\text{C min}^{-1}$  under a nitrogen flow rate of  $50 \text{ mL min}^{-1}$ .

Scanning electron microscopy (SEM). The sample was attached to a horizontal specimen holder with carbon tape and sputtered using a magnetron sputtering system (E-1030 Hitachi, Ltd.). The sputtering conditions were an Au/Pd target with a vacuum of 6 Pa, a discharge current of 15 mA, and a sputtering time of 30 s to achieve a film thickness of 5 nm. Then, measurements were made using a scanning electron microscope (JSM-6510LV JEOL) at an acceleration voltage of 10 kV.

Density and porosity calculation. The porosity of the CNF sheet was measured as follows: 10 circles of 5 mm diameter were punched out of the CNF sheet with a two-hole punch. The weight of each was measured, from which the density was determined. The porosity (Porosity: P %) was then calculated using the Equation (1) [19]:

$$P = \left( 1 - \frac{\rho_m}{\rho_i} \right) \times 100 \quad (1)$$

where  $\rho_i$  is the theoretical density of CNF of  $1500 \text{ kg/m}^3$  and  $\rho_m$  is the density of the CNF sheet measured in this study.

Tensile test. Test specimens were prepared using a specimen punching machine (IMC-1948 type) (Imoto Mfg. Co., Ltd., Takaoka, Japan). Tensile tests were performed using a compact table-top testing machine EZ Test EZ-SX 200 N (Shimadzu Corporation) at a tensile speed of 5 mm/min, referring to JISK7162-AB.

Flexural test. Flexural tests were conducted to observe the flexural properties of the laminated materials. A 2 mm thick laminate consisting of alternating A-CNF sheets (6 layers) and CAB sheets (12 layers) was prepared. The amount of cross-linker added was 14.3 wt% to the total weight of CNF and CAB. The hot-press processing conditions were as follows: 5 min at 0 kN and 15 min at 20 kN. The tests were performed using the flexural test machine AG-5kN X Plus (Shimadzu Corporation, test), with a bending speed of 1 mm/min.

$^1\text{H-NMR}$ . To confirm the chemical properties of acetylated CAB,  $^1\text{H-NMR}$  measurements were performed at room temperature using a JNM-ECA 600 spectrometer (JEOL Ltd., Tokyo, Japan) in deuterated chloroform ( $\text{CDCl}_3$ ) solvent at the Advanced Research Center, Kanazawa University.

ATR-FTIR spectroscopy. Samples were analyzed using Nicolet iS10 (Thermo Fisher Scientific Inc., Tokyo, Japan) equipped with an attenuated total reflection (ATR) unit. The

number of scans was 64. The ratios of Amide II and NCO vibrations to  $\text{CH}_2$  vibration were calculated using Equations (2) and (3), respectively:

$$\text{Amide II} = \frac{\text{Intensity}_{1570}}{\text{Intensity}_{764}} \quad (2)$$

$$\text{NCO} = \frac{\text{Intensity}_{2248}}{\text{Intensity}_{764}} \quad (3)$$

### 3. Results and Discussion

#### 3.1. CAB/CNF Laminate Preparation

First, the authors prepared a laminated material by combining an untreated CNF sheet and a CAB matrix. However, it was found that some of the specimens delaminated at the interface between CAB and the CNF sheet at the stage of cutting the specimens using a sample punching machine. CNF sheets are known to have a high density in the normal fabrication process. Therefore, when manufacturing a laminate material with a polymer matrix, the polymer is not impregnated. The technique of using highly porous CNF sheets by treating them with acetone is often used. In this study, CNF sheets were also prepared using the acetone treatment method (see Section 2). Table 1 shows the measured density and porosity of untreated CNF and A-CNF. A-CNF sheet shows lower density and higher porosity compared with the untreated one. The difference in the surface condition of the A-CNF sheet and the CNF sheet without acetone treatment was observed by SEM. Figure 2 highlights the results of SEM observation. The untreated CNF sheet was densely packed with fibers, and no pores could be seen from the SEM image. On the other hand, the A-CNF sheet was found to be more porous, with pores the size of several tens of microns. Moreover, since commercial bamboo CNFs are low defibrillated, both nano and microfibrils can be observed. Jonoobi et al. [20] reported that the CNF nanofiber network prepared with acetone is open and porous and the measured porosity was 67%. Furthermore, in this study, we used A-CNF for the preparation of laminated material.

**Table 1.** Density and porosity values for CNF sheets prepared using different methods.

	Density: $\rho_m/\text{kg/m}^3$	Porosity/%
Untreated CNF sheet	878.7	41.4
Acetone-treated CNF sheet	677.8	58.1

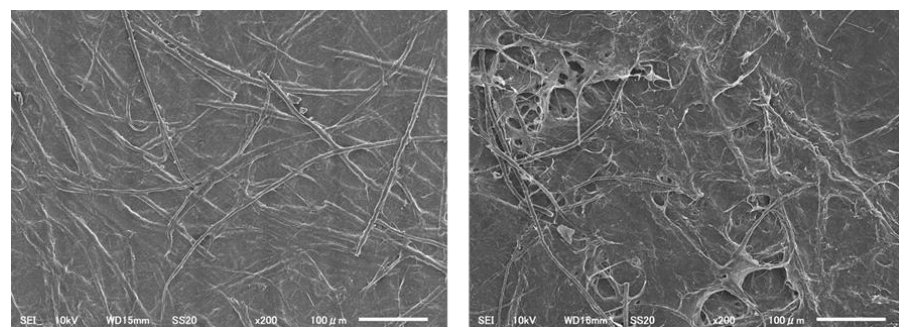


**Figure 2.** SEM images of untreated CNF (left) and A-CNF (right) sheets.

#### 3.2. CAB/A-CNF/D376N Laminate Preparation

Next, to increase the strength of the final material, biomass-derived cross-linking agent polyisocyanurate (D376N) was added. The mechanical strength was measured to determine the appropriate cross-linking material amount and molding process conditions. The mechanical strength of the laminate was first investigated by varying the amount of crosslinking agent. Stress–strain curves obtained from tensile tests are shown in Figure 3.

The elastic modulus results for CAB/A-CNF/D376N cross-linker are shown in Figure S1. The tensile strength increased as the amount of cross-linker increased, and at 14.3 wt% of D376N, the tensile strength was 43.1 MPa, which is 72.4% higher than for neat CAB. The tensile strength remained constant at approximately 43 MPa even when 14.3 wt% or more of D376N was added. Cross-linking agent D376N contains three isocyanate groups. Although it can form a cyclic structure with hydroxyl groups on the same surface of CNF, remaining isocyanate groups can cross-link with other CNF surface hydroxyl groups and residual hydroxyl groups in CAB. The elastic modulus also showed a similar trend. From this experiment, it was found that 14.3 wt% of cross-linking material is the most optimal amount for developing a high-strength laminate. Further increase of the cross-linker amount from 14.3 wt% to 24.5 wt% does not significantly improve the tensile strength. In another work, [16] prepared CAB/CNC composite by feeding the reinforcement as suspension during extrusion. They reported similar tensile strength results (40 MPa) for CAB/CNC with only 5% CNC. Acetone treatment of CNF increases the porosity but can decrease the strength of the bonds between CNF fibers and even between the CAB and the fibers [20]. The thermal property of CAB/A-CNF/D376N with 14.3 wt% of cross-linker was measured (Figure S2). The obtained composite shows good thermal stability. The temperature of 5% mass loss ( $T_{d5\%}$ ) was 308 °C.

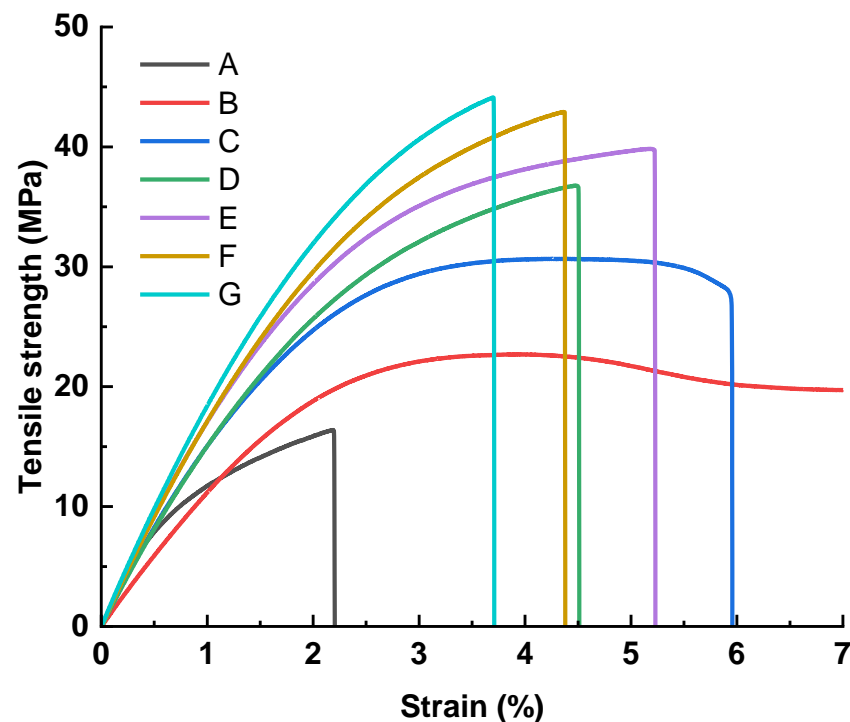


**Figure 3.** Tensile strength–strain behavior of laminated CAB/CNF with different amounts of cross-linker D376N. Samples: (A) A-CNF; (B) CAB500-5; (C) CAB/A-CNF/D376N (0 wt%); (D) CAB/A-CNF/D376N (3.9 wt%); (E) CAB/A-CNF/D376N (7.7 wt%); (F) CAB/A-CNF/D376N (14.3 wt%); (G) CAB/A-CNF/D376N (24.5 wt%).

### 3.3. Influence of Hot-Press Time

Next, the effect of varying the hot-press time was subsequently investigated: the amount of D376N was 14.3 wt%, as determined in the previous experiment, and the hot-press pressure was 20 kN. The obtained stress–strain curve is shown in Figure 4. The elastic modulus obtained from these curves is shown in Figure S3. The tensile strength was slightly lower for the hot-press time of 5 min, but the values for 15 min and longer were close. The same trend was observed for the elastic modulus. From the above, the authors conclude that 15 min of hot-press time is sufficient. In the literature, the reaction time between cellulose and different isocyanates varies largely depending on the type of

isocyanate and the reaction solvent system [21]. Moreover, there are no changes in the color of the composite material for 15 min of hot-press time. The color changes are observed starting from 35 min of hot pressing (Table S2). The degradation of wood particles can take place at high temperatures for a long hot-press time [22].

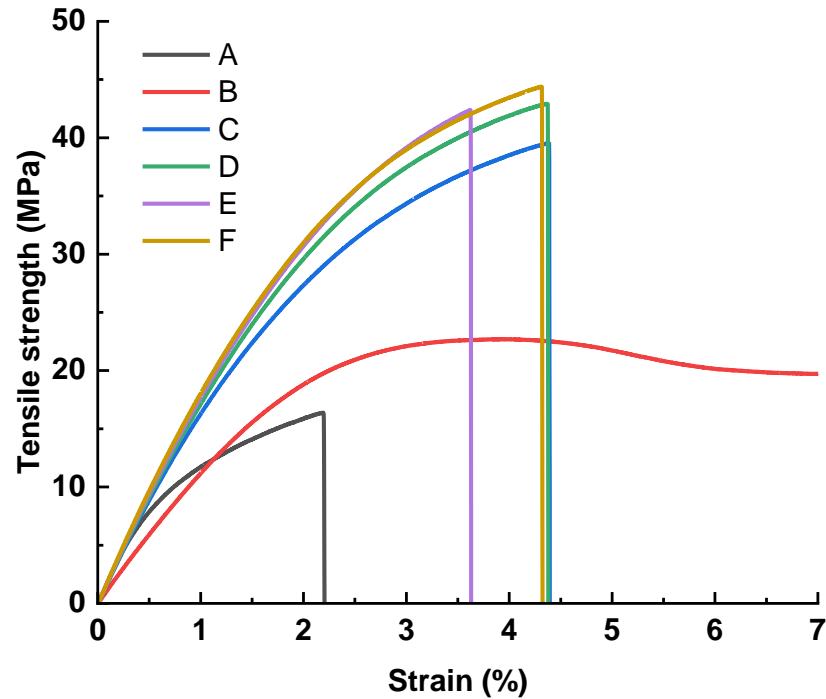


**Figure 4.** Tensile strength–strain behavior of laminated CAB/CNF/D376N for different hot-press time. Samples: (A) A-CNF; (B) CAB500-5; (C) CAB/A-CNF/D376N 5 min; (D) CAB/A-CNF/D376N 15 min; (E) CAB/A-CNF/D376N 25 min; (F) CAB/A-CNF/D376N 35 min.

3.4. Influence of Hot-Press Pressure

Finally, the effect of varying the hot-press pressure was investigated. Based on previous experimental results, the amount of cross-linker was 14.3 wt% and the hot-press time was 15 min. Tensile strength and elastic modulus are presented in Figure 5 and Figure S4. The tensile strength results for the one with 0 kN hot-press pressure were lower than the others. This is considered to be due to the weak adhesion of CAB to A-CNF because no pressure was applied. On the other hand, those with 10 kN pressure, 20 kN pressure, and 40 kN pressure showed almost the same values of 43.9 MPa, 43.1 MPa, and 43.4 MPa, respectively, indicating that the hot-press pressure should be 10 kN or higher. The elastic moduli of all composite material samples were similar to the elastic modulus of A-CNF (1.93 GPa).

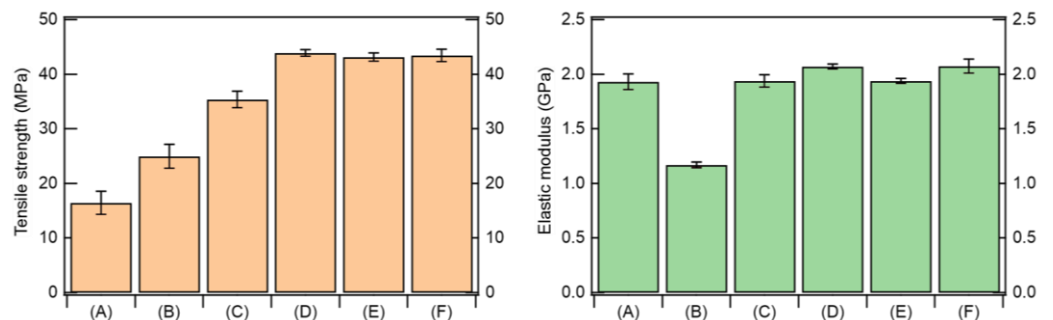


**Figure 5.** Tensile strength (left) and elastic modulus (right) results of laminated CAB/A-CNF/ D376N for different hot-press pressure. Samples: (A) A-CNF; (B) CAB500-5; (C) CAB/A-CNF/D376N 0 kN; (D) CAB/A-CNF/D376N 10 kN; (E) CAB/A-CNF/D376N 20 kN; (F) CAB/A-CNF/D376N 40 kN.

### 3.5. Flexural Test Results

The flexural properties of neat CAB and CAB-based laminates were examined. The obtained flexural force–displacement curve is shown in Figure 6. The calculated flexural strength of CAB alone was 45.4 MPa, and that of the laminate of CAB and A-CNF was 45.6 MPa, showing no difference. However, when D376N was added as a cross-linking agent, the flexural strength was 52.8 MPa, 16.3% higher than that of neat CAB. These results may be attributed to the improved interfacial shear strength due to the cross-linking of the CAB/A-CNF interface by D376N. Furthermore, the CAB/A-CNF/D376N sample shows higher flexural modulus compared with CAB and CAB/A-CNF samples. This indicates the higher stiffness of the composite material. Improved interfacial bonding between the CNF and CAB facilitates load transfer. Finally, from Figure S5 it can be seen that there was no fracture observed for the CAB/A-CNF composite. In contrast, CAB/A-CNF/D376N was completely or partially fractured. This indicates that the addition of the cross-linking agent made the material brittle.

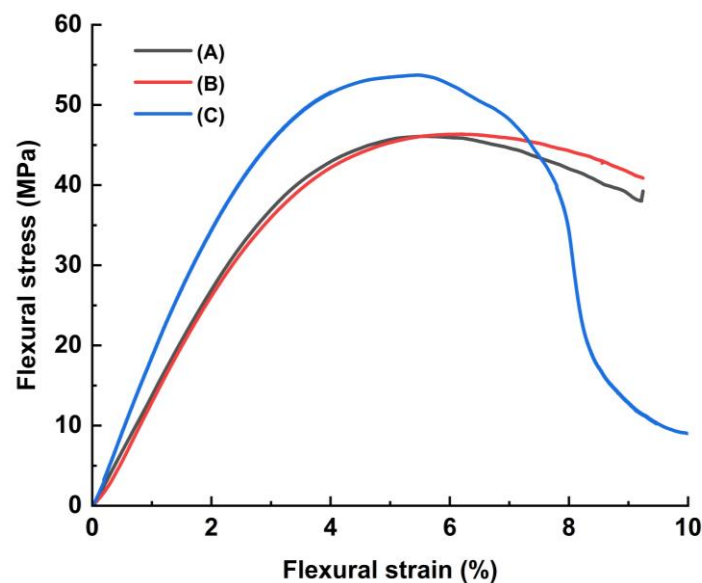


**Figure 6.** Flexural stress—strain behavior of laminates. Samples: (A) CAB; (B) CAB/A-CNF; (C) CAB/A-CNF/D376N.

### 3.6. Investigation of Cross-Linking between CNFs

We investigated whether the addition of a cross-linking agent causes cross-linking between CNFs. FTIR spectra were measured to confirm the formation of urethane bonds. The results of the FTIR measurements are shown in Figure 7. For both samples (before and after the reaction),  $\text{CH}_2$  angular vibration at  $764\text{ cm}^{-1}$ , amide II at  $1570\text{ cm}^{-1}$ , and NCO stretching vibration at  $2248\text{ cm}^{-1}$  were observed. The intensity ratio of NCO to  $\text{CH}_2$  (Equation (3)) after the reaction decreased compared with that before the reaction, while the intensity ratio of amide II increased (Equation (2)), confirming the formation of a urethane bond between the A-CNF/cross-linker. This is in good agreement with previously published data on cellulose cross-linking with isocyanate reagents [23]. Furthermore, the results of the tensile test (Figure S6) show that the tensile strength of the A-CNF sheet alone was 16.5 MPa, while that of the A-CNF/D376N was 36.2 MPa, an improvement of 119%. The elastic modulus was also improved by 40.4%, from 1.93 GPa to 2.71 GPa, which confirms the reaction between the cross-linker and A-CNF surface.



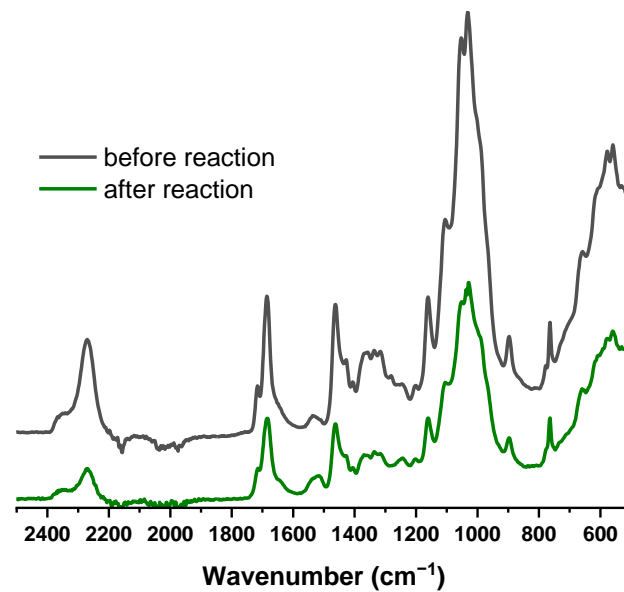


Figure 7. FTIR spectra before and after the reaction of A-CNF/D376N.

### 3.7. Confirmation of Cross-Linking Reaction at the CAB/A-CNF Interface

To investigate the reaction on the interface between CAB and A-CNF, CAB with DS of 3 was synthesized by acetylation of neat CAB500-5 with DS 2.75 (Materials and Methods). Synthesis was confirmed by  $^1\text{H-NMR}$  and FTIR (Figure S7 and Figure S8, respectively). The tensile strength of the two polymers CAB500-5 (DS 2.75) and CAB500-5 (DS 3), the tensile strength of the CAB/A-CNF, and the tensile strength of the CAB/A-CNF/D376N are shown in Figure 8. The tensile strength of the CAB500-5 (DS 3)/A-CNF was 31.2 MPa. The addition of cross-linker increases tensile strength up to 40 MPa, which corresponds to 28% of the increase (CAB500-5 (DS 3)/A-CNF/D376N). Since there are no hydroxyl groups in the CAB500-5 (DS 3), there is no cross-linking at the CAB500-5 (DS 3)/A-CNF interface. Therefore, the improvement of tensile strength is considered to be due to cross-linking between A-CNF hydroxyl groups, as it was discussed in the previous chapter. In contrast, the tensile strength of CAB500-5 (DS 2.75)/A-CNF/D376N was 43.1 MPa, which was 7.8% higher than that of CAB500-5 (DS 3)/A-CNF/D376N. In this case, the enhancement in tensile strength is due to the cross-linking effect at the CAB/A-CNF interface.

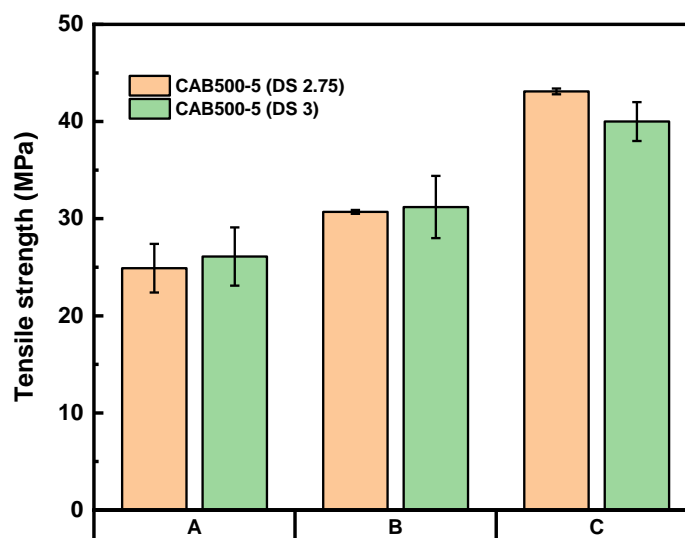


Figure 8. Results of tensile test of laminated material with and without hydroxyl group of CAB. Samples: (A) CAB; (B) CAB/A-CNF; (C) CAB/A-CNF/D376N (14.3 wt%).

#### 4. Conclusions

In this study, cellulose composite material was manufactured by sandwiching CNF reinforcement filler between CAB matrices using the hot-press technique. The cross-linking agent polyisocyanurate D376N (STABIO™) was applied to improve the adhesion between the matrix and filler. The obtained composite material exhibits improved mechanical properties (tensile strength and flexural strength) compared with neat CAB. The optimal manufacturing conditions (cross-linker amount, hot-press pressure, and time) were investigated. It was found that the optimal amount of D376N is 14.3 wt% to make a high-strength CAB/A-CNF/D376N laminated material. It was also shown that a hot-press time of 15 min and hot-press pressure of 10 kN are necessary for the molding process. Finally, it was shown that the improved mechanical properties of the CAB/A-CNF composite are due to cross-linking between A-CNF fibers as well as a reaction at the interface of CAB and A-CNF. The results from this work show the great potential of cellulose-based composite materials in terms of high mechanical performance. Cross-linking using bio-based chemicals can be a suitable way to improve the compatibility between different components of bionanocomposites.

**Supplementary Materials:** The following supporting information can be downloaded at: <https://www.mdpi.com/article/10.3390/jcs7030130/s1>.

**Author Contributions:** Conceptualization, N.W. and K.T.; methodology, K.Y., R.M., N.W. and G.S.; validation, R.S., T.F., N.W. and K.T.; formal analysis, K.Y.; investigation, K.Y. and R.M.; resources, R.S. and E.R.D.I.; writing—original draft preparation, R.M.; writing—review and editing, all authors; supervision, T.F., N.W. and K.T.; project administration, N.W. and K.T.; funding acquisition, N.W. and K.T. All authors have read and agreed to the published version of the manuscript.

**Funding:** This work was funded by the Japan Science and Technology Agency (JST) (grant number JPMJPF2102 for K.T.) and the Japan Society for the Promotion of Science (JSPS) KAKENHI (grant numbers 18H02253 and 22H02404 for K.T.; 21K05704 for N.W.).

**Data Availability Statement:** Data are available upon request.

**Conflicts of Interest:** The authors declare no conflict of interest.

#### References

1. Andrew, J.J.; Dhakal, H.N. Sustainable biobased composites for advanced applications: Recent trends and future opportunities—A critical review. *Compos. Part C Open Access* **2022**, *7*, 100220. [CrossRef]
2. Jonoobi, M.; Mathew, A.P.; Abdi, M.M. A Comparison of Modified and Unmodified Cellulose Nanofiber Reinforced Polylactic Acid (PLA) Prepared by Twin Screw Extrusion. *J. Polym. Environ.* **2012**, *20*, 991–997. [CrossRef]
3. Wu, J.; Dong, Z.; Li, X.; Li, P.; Wei, J.; Hu, M.; Geng, L.; Peng, X. Constructing acid-resistant chitosan/cellulose nanofibrils composite membrane for the adsorption of methylene blue. *J. Environ. Chem. Eng.* **2022**, *10*, 107754. [CrossRef]
4. Drzal, L.T.; Madhukar, M. Fibre-matrix adhesion and its relationship to composite mechanical properties. *J. Mater. Sci.* **1993**, *28*, 569–610. [CrossRef]
5. Dufresne, A. Processing of Polymer Nanocomposites Reinforced with Polysaccharide Nanocrystals. *Molecules* **2010**, *15*, 4111–4128. [CrossRef] [PubMed]
6. Her, K.; Jeon, S.H.; Lee, S.; Shim, B.S. Esterification of Cellulose Nanofibers with Valeric Acid and Hexanoic Acid. *Macromol. Res.* **2020**, *28*, 1055–1063. [CrossRef]
7. Beaumont, M.; Winklehner, S.; Veigel, S.; Mundigler, N.; Gindl-altmutter, W.; Potthast, A.; Rosenau, T. Simple process to surface-acetylated cellulose. *Green Chem.* **2020**, *22*, 5605–5609. [CrossRef]
8. Navarro, J.R.G.; Edlund, U. Surface-Initiated Controlled Radical Polymerization Approach to Enhance Nanocomposite Integration of Cellulose Nanofibrils. *Biomacromolecules* **2017**, *18*, 1947–1955. [CrossRef]
9. Roy, D.; Guthrie, J.T.; Perrier, S. Graft Polymerization: Grafting Poly(styrene) from Cellulose via Reversible Addition–Fragmentation Chain Transfer (RAFT) Polymerization. *Macromolecules* **2005**, *38*, 10363–10372. [CrossRef]
10. Goussé, C.; Chanzy, H.; Cerrada, M.L.; Fleury, E. Surface silylation of cellulose microfibrils: Preparation and rheological properties. *Polymer* **2004**, *45*, 1569–1575. [CrossRef]
11. Abdelmouleh, M.; Boufi, S.; Belgacem, M.N.; Duarte, A.P.; Ben Salah, A.; Gandini, A. Modification of cellulosic fibres with functionalised silanes: Development of surface properties. *Int. J. Adhes. Adhes.* **2004**, *24*, 43–54. [CrossRef]
12. Laitinen, O.; Suopajarvi, T.; Österberg, M.; Liimatainen, H. Hydrophobic, Superabsorbing Aerogels from Choline Chloride-Based Deep Eutectic Solvent Pretreated and Silylated Cellulose Nanofibrils for Selective Oil Removal. *ACS Appl. Mater. Interfaces* **2017**, *9*, 25029–25037. [CrossRef] [PubMed]

13. Ansari, F.; Berglund, L.A. Toward Semistructural Cellulose Nanocomposites: The Need for Scalable Processing and Interface Tailoring. *Biomacromolecules* **2018**, *19*, 2341–2350. [[CrossRef](#)]
14. Szabó, L.; Milotskyi, R.; Fujie, T.; Tsukegi, T.; Wada, N.; Ninomiya, K.; Takahashi, K. Short Carbon Fiber Reinforced Polymers: Utilizing Lignin to Engineer Potentially Sustainable Resource-Based Biocomposites. *Front. Chem.* **2019**, *7*, 757. [[CrossRef](#)] [[PubMed](#)]
15. Lee, J.E.; Shim, S.B.; Park, J.H.; Chung, I. Interfacial Properties and Melt Processability of Cellulose Acetate Propionate Composites by Melt Blending of Biofillers. *Polymers* **2022**, *14*, 4286. [[CrossRef](#)] [[PubMed](#)]
16. Bondeson, D.; Syre, P.; Niska, K.O. All cellulose nanocomposites produced by extrusion. *J. Biobased Mater. Bioenergy* **2007**, *1*, 367–371. [[CrossRef](#)]
17. Wada, N.; Fujie, T.; Sasaki, R.; Matsushima, T.; Takahashi, K. Direct synthesis of a robust cellulosic composite from cellulose acetate and a nanofibrillated bacterial cellulose sol. *Polym. J.* **2022**, *54*, 735–740. [[CrossRef](#)]
18. Oksman, K.; Aitomäki, Y.; Mathew, A.P.; Siqueira, G.; Zhou, Q.; Butylina, S.; Tanpichai, S.; Zhou, X.; Hooshmand, S. Review of the recent developments in cellulose nanocomposite processing. *Compos. Part A Appl. Sci. Manuf.* **2016**, *83*, 2–18. [[CrossRef](#)]
19. Henriksson, M.; Berglund, L.A.; Isaksson, P.; Lindström, T.; Nishino, T. Cellulose nanopaper structures of high toughness. *Biomacromolecules* **2008**, *9*, 1579–1585. [[CrossRef](#)]
20. Jonoobi, M.; Aitomäki, Y.; Mathew, A.P.; Oksman, K. Thermoplastic polymer impregnation of cellulose nanofibre networks: Morphology, mechanical and optical properties. *Compos. Part A Appl. Sci. Manuf.* **2014**, *58*, 30–35. [[CrossRef](#)]
21. Abushammala, H.; Mao, J. A Review of the Surface Modification of Cellulose and Nanocellulose Using Aliphatic and Aromatic Mono- and Di-Isocyanates. *Molecules* **2019**, *24*, 2782. [[CrossRef](#)] [[PubMed](#)]
22. Winandy, J.E.; Krzysik, A.M. Thermal degradation of wood fibers during hot-pressing of MDF composites. Part I, Relative effects and benefits of thermal exposure. *Wood Fiber Sci.* **2007**, *39*, 450–461.
23. Stenstad, P.; Andresen, M.; Tanem, B.S.; Stenius, P. Chemical surface modifications of microfibrillated cellulose. *Cellulose* **2008**, *15*, 35–45. [[CrossRef](#)]

**Disclaimer/Publisher’s Note:** The statements, opinions and data contained in all publications are solely those of the individual author(s) and contributor(s) and not of MDPI and/or the editor(s). MDPI and/or the editor(s) disclaim responsibility for any injury to people or property resulting from any ideas, methods, instructions or products referred to in the content.